NANO LETTERS

2004
Vol. 4, No. 8
1547−1550

Synthesis of Single-Crystalline $La_{1-x}Ba_xMnO_3$ Nanocubes with Adjustable Doping Levels

Jeffrey J. Urban, Lian Ouyang, Moon-Ho Jo, Dina S. Wang, and Hongkun Park*

Department of Chemistry and Chemical Biology, Harvard University, 12 Oxford Street, Cambridge, Massachusetts 02138

Received May 16, 2004; Revised Manuscript Received July 1, 2004

ABSTRACT

We report a hydrothermal synthesis of single-crystalline nanocubes composed of lanthanum barium manganite ($La_{1-x}Ba_xMnO_3$) with three different doping levels ($x = 0.3$, 0.5, and 0.6). The synthesis yields clearly faceted nanocubes with a pseudo-cubic perovskite structure. Typical nanocubes have sizes ranging between 50 and 100 nm irrespective of doping level. Magnetic measurements performed on nanocube ensembles show that the magnetic properties depend on the doping level. The ability to synthesize nanoscale manganites of a desired doping level should enable detailed investigations of the size-dependent evolution of magnetism, colossal magnetoresistance, and nanoscale phase separation.

Since the discovery of colossal magnetoresistivity (CMR),[1,2] mixed valence manganites have received considerable attention from the scientific community.[1−6] The interplay among the spin, charge, and orbital degrees of freedom in these materials[3−6] leads to a host of phenomena that are yet poorly understood, such as metal−insulator transitions (MIT), magnetic phase transitions, and nanoscale charge and orbital ordering.[1−9] A particularly important material parameter that causes transitions among these distinct phases is the variable chemical doping of the parent manganites.

Nanocrystalline materials typically exhibit physical and chemical properties that are distinct from their bulk counterparts.[10,11] The properties of mixed valence manganites are also expected to depend on material size due to both the nanoscale phase inhomogeneity inherent to bulk materials and additional surface effects.[7−9,12−16] Indeed, previous investigations on thin-film manganite samples have shown that their properties depend sensitively on the film thickness, leading to surface-induced phase separation[7−9] and strain-dependent MIT.[13] Although advances have been made in the preparation of nano- and microcrystalline oxides including manganites,[17−25] detailed physical investigations of nanocrystalline manganites have not been possible due to the lack of reliable methods to prepare well-isolated manganite nanocrystals with variable chemical doping.

Here we report a hydrothermal preparation of a series of lanthanum barium manganite (LBMO) nanocubes whose barium content is varied controllably. Specifically, we present the synthesis of $La_{1-x}Ba_xMnO_3$ nanocubes with $x = 0.3$, 0.5, and 0.6, which span three distinct regions of the LBMO phase diagram.[26] The synthesis yields single-crystalline nanocubes with clearly faceted edges whose typical sizes range from 50 to 100 nm. Measurements performed on nanocube ensembles show that their magnetic properties depend strongly on chemical doping.

One important control parameter in the synthesis of mixed valence manganites with adjustable doping levels is the average oxidation state of the Mn ion. In the present synthesis, the control over the Mn oxidation state is achieved by changing the ratio of two Mn precursors, $KMnO_4$ and $MnCl_2$, that contain Mn ions with distinct initial oxidation states.[22] The synthetic procedure for $La_{0.7}Ba_{0.3}MnO_3$ nanocubes is described below as an example. A similar procedure can also be applied for other doping levels as long as the molarity of KOH is adjusted for each composition to accommodate inherent differences in lanthanum and barium ion reactivity (see below).

In a typical synthesis of $La_{0.7}Ba_{0.3}MnO_3$ nanocubes, 1.11 mmol of $MnCl_2 \cdot 4H_2O$ (Aldrich, 99.99%), 0.39 mmol of $KMnO_4$ (Aldrich, 99+%), 1.05 mmol of $La(NO_3)_3 \cdot 6H_2O$ (Aldrich, 99.99%), and 0.45 mmol of $Ba(OH)_2 \cdot 8H_2O$ (Aldrich, 98+%) were mixed in doubly distilled water (total reaction volume ~15 mL). The solution was made strongly alkaline by saturating it with KOH (Aldrich, 99.99%) and loaded into a 45-mL hydrothermal cell (Parr Instruments, Moline, IL). The reaction was performed by heating the cell to 300 °C under autogenous pressure for 24 h. After the hydrothermal cell was cooled, the supernatant liquid was discarded and the remaining product was washed with water

* Corresponding author. E-mail: HPark@chemistry.harvard.edu.

10.1021/nl049266k CCC: $27.50
Published on Web 07/16/2004

and dried in ambient conditions at 120 °C. The reaction produced a highly crystalline black powder composed of LBMO nanocube aggregates. Isolated nanocubes were obtained by first sonicating the reaction product in water (∼1 mg/mL) and then passing the solution through a 0.45-mm filter to remove any aggregates that remain undispersed. The size distribution of the nanocubes could be tightened by suspending ∼4 mg of the reaction product in 8 mL of *o*-dichlorobenzene by sonication and then adding 1 mL of methanol to preferentially drop out larger nanocubes.

The molarity of KOH affects the chemical composition as well as morphology of the reaction product.[22,27] The optimum [KOH] that yields pure LBMO samples decreases with increasing barium content of LBMO: specifically, the optimum [KOH] values are found to be [KOH] = 18, 12, and 8 M for $x = 0.3$, 0.5, and 0.6, respectively. When [KOH] < 18 M for $x = 0.3$, the reaction produced a mixture of LBMO nanocubes and $La(OH)_3$ nanorods.[27] For $x = 0.5$ and 0.6, the reaction yielded a mixture of LBMO nanocubes and $BaMnO_3$ particles when the [KOH] deviated from the optimal values appreciably. It is important to note that the synthesis of $La_{0.5}Ba_{0.5}MnO_3$ nanowires that were reported previously[21,25] could not be reproduced in our laboratory despite the similarity of the reaction conditions: indeed, the only nanostructures with nanowire morphology generated in the reaction were $La(OH)_3$ nanorods (see Supporting Information).[27]

Representative transmission electron microscope (TEM) and scanning electron microscope images of the reaction product are shown in Figure 1 and Supporting Information. These images clearly reveal that the products are nanometer-sized cubes for all doping levels, with typical sizes of 50∼100 nm. The size distribution is rather broad, however, and nanocubes as small as 20 nm or as big as ∼500 nm could be found in nascent reaction products. High-resolution TEM (HRTEM) and selected area diffraction analyses were performed on many cubes of each composition. These studies indicate that, irrespective of doping level, individual nanocubes are single crystalline and possess sharp {100} faceted edges, as illustrated in Figure 1b. Analysis of electron-diffraction from individual nanocubes and powder X-ray diffraction (XRD) patterns from nanocube ensembles, such as those shown in Figure 2, indicates that manganite nanocubes of all three compositions are highly crystalline and share the pseudo-cubic perovskite structure. The lattice parameters of $La_{1-x}Ba_xMnO_3$ nanocubes determined from XRD analyses are 3.89, 3.95, and 3.95 Å for $x = 0.3$, 0.5, and 0.6, respectively, in agreement with the lattice parameters of bulk materials with the same doping levels.[26] It should be noted that the small rhombohedral distortions seen in bulk materials are not discernible in any of the nanocube samples reported here. The rhombohedral distortion in these nanocube samples may be obscured by a broadening of the XRD peaks caused by surface strain, although further investigations are necessary to clarify this issue (see Supporting Information for full XRD analysis).

To assess the stoichiometry of nanocube samples, energy-dispersive X-ray spectrometry was performed on individual

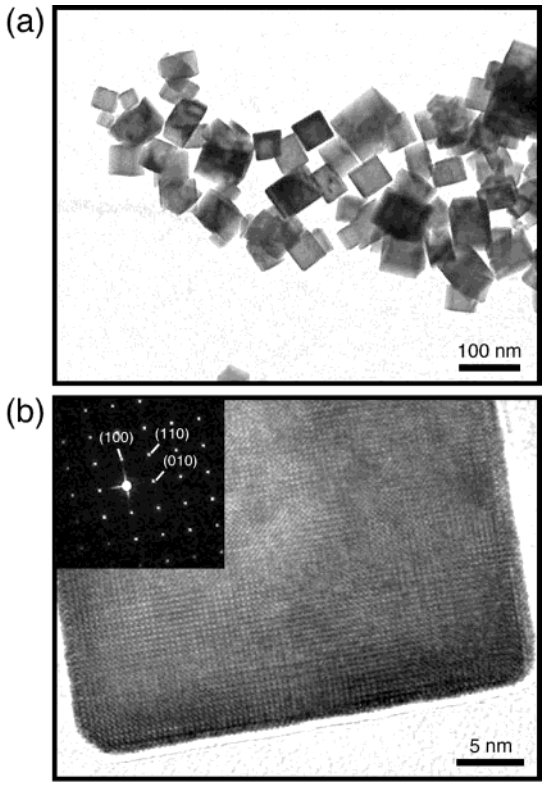

Figure 1. (a) Transmission electron microscopy (TEM) image of $La_{0.5}Ba_{0.5}MnO_3$ nanocubes, illustrating that the reaction produces isolated nanocubes ranging from 20 to 500 nm in size. Low-resolution TEM images for other doping levels are indistinguishable. (b) High-resolution TEM image of a 30-nm $La_{0.7}Ba_{0.3}MnO_3$ nanocube along with a selected area diffraction pattern shown in the inset.

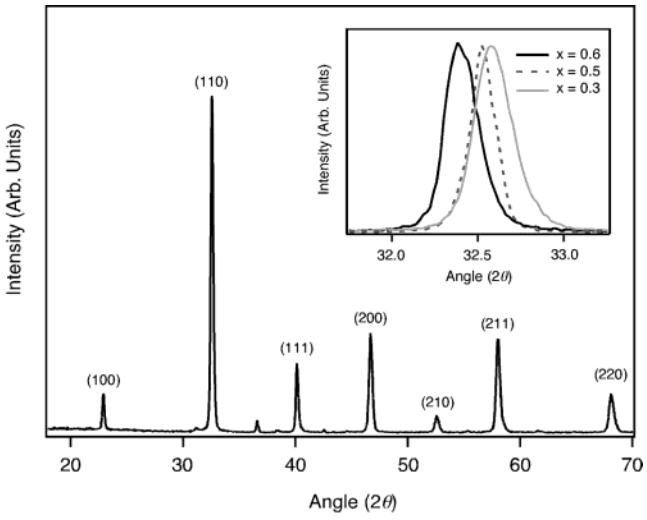

Figure 2. Powder X-ray diffractogram of the $La_{1-x}Ba_xMnO_3$ ($x = 0.3$) nanocubes with pseudo-cubic crystallographic assignments. The diffractogram shows that the nanocubes have the same crystalline symmetry as bulk $La_{1-x}Ba_xMnO_3$. The inset shows the (110) diffraction peaks of the samples for all three compositions ($x = 0.3$, 0.5, and 0.6), illustrating the slight gradual increase in lattice parameter observed as a function of barium doping.

$La_{1-x}Ba_xMnO_3$ nanocubes using a high-resolution TEM operating in a scanning TEM mode. In every nanocube analyzed, La, Ba, Mn, and O were present in the correct

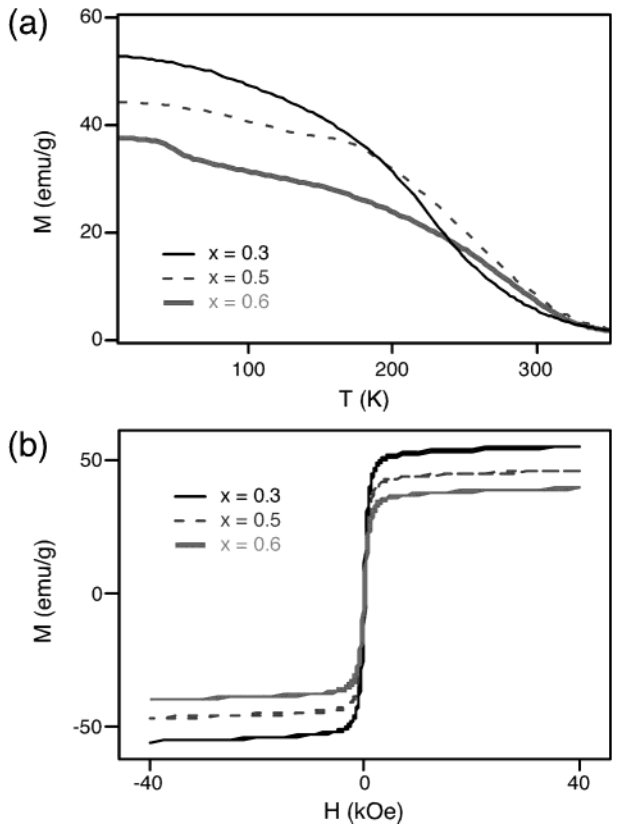

Figure 3. (a) Plot of magnetization (M) against temperature (T) obtained from $La_{1-x}Ba_xMnO_3$ nanocube ensembles for all three compositions ($x = 0.3$, 0.5, and 0.6). The samples were cooled and measured during warming under the applied field of 10 kOe. (b) Plot of M as a function of applied magnetic field (H) measured at 10 K for $La_{1-x}Ba_xMnO_3$ nanocube ensembles for all three compositions ($x = 0.3$, 0.5, and 0.6).

ratios to within instrumental accuracy (see Supporting Information). Atomic absorption measurements performed on powder samples (Galbraith Laboratories, Knoxville, TN) also indicate that the reported metal-ion stoichiometries are accurate to within ±5%.

The magnetic properties of the $La_{1-x}Ba_xMnO_3$ nanocubes were studied by measuring the sample magnetization as a function of applied magnetic field using a superconducting quantum interference device magnetometer. Figure 3a shows magnetization (M) versus temperature (T) curves obtained from nanocube samples of all three compositions. These curves were obtained by cooling each sample to $T = 10$ K and then recording M as the sample was warmed to 350 K under the application of a magnetic field strong enough to saturate the sample magnetization (10 kOe). The results clearly illustrate the occurrence of ferromagnetic-to-paramagnetic phase transitions in all three samples as the temperature is increased. Notably, the magnitude of the low-temperature saturation magnetization decreases with increased barium doping, in accord with the previous bulk measurements.[26] The detailed features of $M-T$ curves previously recorded from bulk samples[24] are reproduced from nanocube samples as well, including the crossing of the $x = 0.3$ and $x = 0.5$ plots at ~200 K and the sharp step in the magnetization of the $x = 0.6$ sample below 100 K.

Figure 3b shows plots of M versus applied magnetic field (H) at $T = 10$ K obtained from nanocube ensembles of all three compositions. All nanocube samples exhibited clear ferromagnetic switching characteristics. It should be noted that the samples in all three compositions exhibit a slight reduction in saturation magnetization as well as a suppression of the phase transition temperature compared to their bulk counterparts. This result may originate from the enhanced surface-to-volume ratio in these nanocrystalline samples or the presence of a superparamagnetic phase in these nanocrystalline samples, although further investigations are necessary to clarify the issue.[13−16] We note that previous results have indicated that perovskite manganites exhibit significantly reduced magnetization at the surface in comparison to the bulk material[14] due to spin disorder at the surfaces in $La_{1-x}Ba_xMnO_3$.[16]

The present study demonstrates that single-crystalline $La_{1-x}Ba_xMnO_3$ nanocubes with an adjustable Ba doping level can be synthesized via hydrothermal methods. The synthesis of these nanocubes should enable the detailed investigation of the size-dependent evolution of nanoscale phase separation, magnetism, and CMR in mixed valence manganites. The synthetic methods presented here may also be adapted to other classes of manganites and perovskite oxides by selecting appropriate precursors.

Acknowledgment. This work is supported by the National Science Foundation (NSF CHE-0134787), the Packard Foundation, and the Dreyfus Foundation. We thank H. L. Ju from Yonsei University for bulk lanthanum barium manganite samples, M. M. Deshmukh, and A. L. Prieto for helpful discussions, and Y. Lu for technical assistance.

Supporting Information Available: Scanning electron microscope images, high resolution TEM images, XRD patterns, energy-dispersive X-ray spectra (EDS), and raw data from elemental analysis of $La_{1-x}Ba_xMnO_3$ nanocubes, bulk $La_{1-x}Ba_xMnO_3$ standards, and $La(OH)_3$ nanowires. This material is available free of charge via the Internet at http://pubs.acs.org.

References

(1) Jin, S.; Tiefel, T. H.; McCormack, M.; Fastnacht, R. A.; Ramesh, R.; Chen, L. H. *Science* **1994**, *264*, 413.
(2) von Helmolt, R.; Wecker, J.; Holzapfel, B.; Schultz, L.; Samwer, K. *Phys. Rev. Lett.* **1993**, *71*, 2331.
(3) Millis, A. J. *Nature* **1998**, *392*, 147.
(4) Moreo, A.; Yunoki, S.; Dagotto, E. *Science* **1999**, *283*, 2034.
(5) Tokura, Y.; Nagaosa, N. *Science* **2000**, *288*, 462.
(6) Salamon, M. B.; Jaime, M. *Rev. Mod. Phys.* **2001**, *73*, 583.
(7) Fath, M.; Freisem, S.; Menovsky, A. A.; Tomioka, Y.; Aarts, J.; Mydosh, J. A. *Science* **1999**, *285*, 1540.
(8) Renner, C.; Aeppli, G.; Kim, B.-G.; Soh, Y.-A.; Cheong, S.-W. *Nature* **2002**, *416*, 518.
(9) Loudon, J. C.; Mathur, N. D.; Midgley, P. A. *Nature* **2002**, *420*, 797.
(10) Alivisatos, A. P. *Science* **1996**, *271*, 933.
(11) Hu, J.; Odom, T. W.; Lieber, C. M. *Acc. Chem. Res.* **1999**, *32*, 435.
(12) Sun, J. Z.; Abraham, D. W.; Rao, R. A.; Eom, C. B. *Appl. Phys. Lett.* **1999**, *74*, 3017.
(13) Zhang, J.; Tanaka, H.; Kanki, T.; Choi, J.-H, Kawai, T. *Phys. Rev. B.* **2001**, *64*, 184404.
(14) Park, J.-H.; Vescovo, E.; Kim, H.-J.; Kwon, C.; Ramesh, R.; Venkatesan, T. *Phys. Rev. Lett.* **1998**, *81*, 1953.

(15) Calderon, M. J.; Brey, L.; Guinea, F. *Phys. Rev. B* **1999**, *60*, 6698.
(16) Solovyev, I. V.; Terakura, K. *Phys. Rev. B* **2001**, *63*, 174425.
(17) Yang, P.; Deng, T.; Zhao, D.; Feng, P.; Pine, D.; Chmelka, B. F.; Whitesides, G. M.; Stucky, G. D. *Science* **1998**, *282*, 2244.
(18) O'Brien, S.; Brus, L.; Murray, C. B. *J. Am. Chem. Soc.* **2001**, *123*, 12085.
(19) Urban, J. J.; Yun, W. S.; Gu, Q.; Park, H. *J. Am. Chem. Soc.* **2002**, *124*, 1186.
(20) Vazquez-Vazquez, C.; Blanco, M. C.; Lopez-Quintela, M. A.; Sanchez, R. D.; Rivas, J.; Oseroff, S. B. *J. Mater. Chem.* **1998**, *8*, 991.
(21) Zhu, D.; Zhu, H.; Zhang, Y. *Appl. Phys. Lett.* **2002**, *80*, 1634.
(22) Spooren, J.; Rumpecker, A.; Millange, F.; Walton, R. I. *Chem. Mater.* **2003**, *15*, 1401.
(23) Schaak, R. E.; Mallouk, T. E. *Chem. Mater.* **2002**, *14*, 1455.
(24) Mao, Y. B.; Banerjee, S.; Wong, S. S. *Chem. Commun.* **2003**, *2003*, 408.
(25) Liu, J.; Wang, H.; Zhu, M.; Wang, B.; Yan, H. *Mater. Res. Bull.* **2003**, *38*, 817.
(26) Ju, H. L.; Nam, Y. S.; Lee, J. E.; Shin, H. S. *J. Magn. Magn. Mater.* **2000**, *219*, 1.
(27) Wang, X.; Li, Y. *Angew. Chem., Int. Ed.* **2002**, *41*, 4790.

NL049266K